



High power microsecond fiber laser at 1.5 μm

SVITLANA PAVLOVA,^{1,2,*}  M. EMRE YAGCI,¹ S. KORAY EKEN,¹
ERSAN TUNCKOL,¹ AND IHOR PAVLOV^{1,2,3}

¹FiberLAST, A.S., Ankara 06800, Turkey

²Institute of Physics of the NAS of Ukraine, Kyiv 03028, Ukraine

³Department of Physics, Middle East Technical University, Ankara 06800, Turkey

*s.pavlov@fiberlast.com.tr

Abstract: In this work, we demonstrate a single frequency, high power fiber-laser system, operating at 1550 nm, generating controllable rectangular-shape μs pulses. In order to control the amplified spontaneous emission content, and overcome the undesirable pulse steepening during the amplification, a new method with two seed sources operating at 1550 nm and 1560 nm are used in this system. The output power is about 35 W in CW mode, and the peak power is around 32 W in the pulsed mode. The repetition rate of the system is tunable between 50 Hz to 10 kHz, and the pulse duration is adjustable from 10 μs to 100 μs , with all on the fly electronically configurable design. The system demonstrates excellent long and short time stability, as well as spectral and spatial beam quality.

© 2020 Optical Society of America under the terms of the [OSA Open Access Publishing Agreement](#)

1. Introduction

Nowadays, the fiber laser technology at 1.5 μm wavelengths is not only limited to telecom demands but widely used for various scientific and industrial applications: micromachining and material subsurface modification [1,2], remote sensing [3], range finding and LIDAR systems [4]. In general, all efforts in the development of high power fiber laser systems operating at 1.5 μm can be divided into three main trends according to the operational type: CW mode, which is mainly used for coherent detection type LIDAR systems; short-pulse operation in nano-picosecond range, with the applications in LIDARs, 2D and 3D material processing; and ultrashort pulse operation in femtosecond range for different, mainly research applications. Due to relatively smaller absorption cross-section of Er ions compared to Yb at the conventional pump wavelength, and difficulty to achieve high doping concentration of Er ions inside of the core of the silica fibers, the Er-Yb co-doped fibers are widely used for almost all high power laser systems operating in the vicinity of 1550 nm.

For CW operation, the highest achieved power reported so far is 297 W [5]. There are several other impressive results such as 56.4 W [6] achieved with pumping at conventional wavelength 976 nm, 264 W [7] achieved with in-band pumping at 1535 nm, 100 W [8] and 207 W [9] achieved with pumping at 940 nm.

Some of the recent developments of the fiber lasers with a pulse duration of a few nanoseconds at a low repetition rate have been reported to date: 3.5 ns and 9 W at 100 kHz [10], 140-100 μJ at 25-100 kHz with pulse duration 4-15 ns [11]. For ns operation, master oscillator power amplifier (MOPA) design is commonly used, where the master oscillator is semiconductor distributed feedback (DFB) or Distributed Bragg Reflector (DBR) laser diode. It allows on the fly electronically configurable design of the laser, with adjustable repetition rate and pulse duration. Such a concept is hard to apply directly, if the rectangular shape μs pulses are required, especially at low repetition rate, due to several reasons where the main are the pulse steepening during the amplification and significant amplified spontaneous emission (ASE) growth. Lasers with μs pulse duration are suitable for special material processing, coherent detection sources (trace

gas detection) [12], CO₂ LIDAR system [13], however up to date there are much less number of works conducted to the development of such systems at 1550 nm.

In this work, we demonstrate high power Er-Yb fiber laser system, operating at 1550 nm, with a controllable rectangular shape pulse with a duration of 10 -100 μ s. The repetition rate of the system is tunable between 50 Hz to 10 kHz. To remove undesirable ASE growth, and prevent the pulse steepening during the amplification, we applied a new approach which is based on the use of two seed sources operating at a different wavelength, where the first one is the main seed source operating at 1550 nm, and the second one is a sacrificial seed source. The sacrificial seed source prevents ASE growth by saturating the amplifier during off-periods, and its amplified power can be spectrally filtered out at the end of the system.

2. Experimental setup and operation of the system in CW mode

The general scheme of the experimental setup is shown in Fig. 1. The laser system consists of a seed source, two pre-amplifiers (PA1, PA2), and the main amplifier (MA). The seed source is DFB laser diode which can deliver up to 100 mW power in CW mode at central wavelength 1550 nm, with 1 MHz linewidth. The output signal of the seed source (around 95 mW) was delivered to the first pre-amplifier (PA1). PA1 is based on a double-clad (DC) Er-Yb doped gain fiber with a 10 μ m core diameter. The multimode pump radiation (4 W at 976 nm) was delivered to the first amplifier by a Multimode Pump Combiner (MPC). The optimal output power of PA1 was 1.3 W, demonstrating about 30 % pump to signal conversion efficiency. The second stage (PA2) consisted of the same DC Er-Yb fiber and was backward pumped by 915 nm multimode pump diode through MPC. The output power of PA2 was 7 W at a pump power of 25 W, demonstrating nearly the same 30 % efficiency. When the output power reaches more than 7 W, the parasitic ASE at 1050 nm starts to be observable. Due to lower pump absorption at 915 nm compared to 976 nm the length of the gain fiber in PA2 is kept longer concerning PA1. Although for CW operation it is not necessary to use two preamplifiers in the system, and 7 W of the signal power can be obtained directly by one pre-amplifier, however, due to the low average power of the seed source in the pulsed mode, the use of PA1 is necessary to saturate PA2.

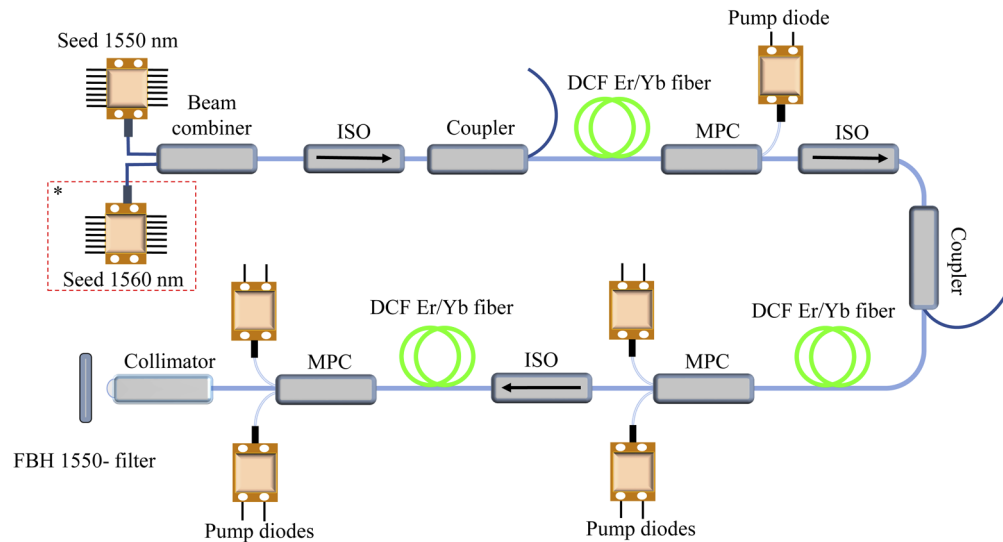


Fig. 1. Schematic of Er-Yb microsecond laser system.

The final section of the laser system MA consists of large mode area Er-Yb co-doped fiber with a core diameter of 25 μ m, which is also backward pumped in the cladding by several high-power

multimode diodes operating at 915 nm. We achieved about 37 W average power (see explanation below) at 96 W of pump power, which corresponds to nearly 40 % pump to signal conversion efficiency. The output of the system was delivered through a high power fiber collimator, which was spliced to the output port of MPC. The active fiber of the MA was placed on an aluminum heat sink and actively cooled by air fans. Before every amplifier, single-mode fiber isolators have been used to protect the amplifiers from backward-propagating light. Besides, a piece of single clad passive fiber with 16- μm core and 250- μm cladding diameters is spliced before the gain fiber of MA, which acts as a simple and effective mode field adapter and cladding mode stripper at the same time. The output spectra after each amplifier stages are depicted in Fig. 2.

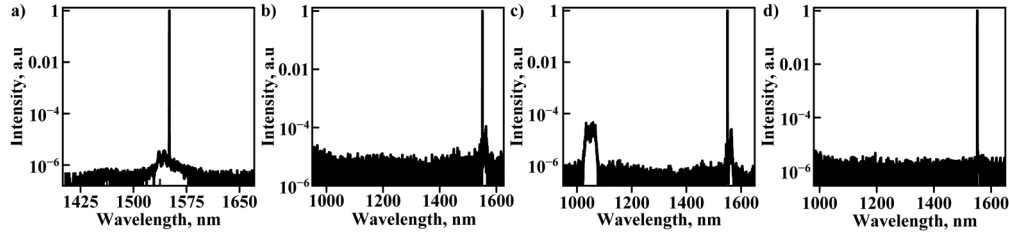


Fig. 2. Output spectra in CW mode: a) first pre-amplifier b) second pre-amplifier c) final amplifier without filter d) final amplifier with filter.

As can be seen from Fig. 2(c), the output spectrum of the final amplifier contains a certain amount of amplified spontaneous emission (ASE) near 1050 nm (about 7 %) and near 1550 nm (about 1%) which was suppressed by free-space narrow band-pass filter, placed in front of the output collimator. The main role of this filter will be described below. The output power after the filter decreased to 35 W. The output spectrum after the filter is presented in Fig. 2(d), demonstrating more than 50 dB signal to noise (ASE) ratio.

3. Operation of the system in μs pulsed mode

During the operation of the system in pulsed mode with 10-100 μs pulse duration and the repetition rate between 50 Hz to 10 kHz, two main difficulties are arising from: slow increase of inversion population and uncontrollable ASE growth due to low repetition rate, significant pulse steepening, which leads to decrease pulse duration and completely disturbs the initially rectangular pulse shape.

Besides, at using pulsed pumping (at reasonable pump power) at low repetition rates, due to long relaxation time between Er^3 levels $^4I_{11/2}$ and $^4I_{13/2}$ and relatively long transition time between Yb^3 $^2F_{5/2}$ and Er^3 $^4I_{11/2}$ levels (Fig. 3), the inversion population of Er-Yb fibers increases slowly and reaching steady-state in more than 100 μs after the pump starts, and slowly decreases after the pump stops. It makes difficult to create an inversion population for just a few tens μs in a controllable way. To reduce experimental time and for a detailed analysis of the pump to signal conversion dynamics in Er-Yb co-doped fiber, we performed numerical simulation. The numerical model of propagation and amplification of pulse in multi-amplifiers was described in [14]. The simulation is based on the rate equations of erbium-ytterbium system (see for example [15]):

$$\frac{dN_6}{dt} = W_{46}^p(N_4 - N_6) - \rho_{65}N_6 - K_{tr}(N_6N_1 - N_3N_4) \quad (1)$$

$$\frac{dN_5}{dt} = \rho_{65}N_6 - W_{54}^sN_5 + W_{45}^sN_4 - \sigma_{54}N_5 - K_{tr}(N_5N_1 - N_3N_4) \quad (2)$$

$$\frac{dN_3}{dt} = W_{13}^p(N_1 - N_3) - \rho_{32}N_3 + K_{tr}(N_5N_1 - N_3N_4) + K_{tr}(N_6N_1 - N_3N_4) \quad (3)$$

$$\frac{dN_2}{dt} = \rho_{32}N_3 - W_{21}^s N_2 + W_{12}^s N_1 - \sigma_{21}N_2 \quad (4)$$

$$N_{Er} = N_1 + N_2 + N_3; N_{Yb} = N_4 + N_5 + N_6 \quad (5)$$

where N_n - the number of ions in corresponding state, W_{nm}^p - the probability for absorption and W_{nm}^s - the probability for stimulated emission between the levels n and m , which are depended on pump and signal intensities and corresponding cross-sections $\delta_{nm}^{p,s}$; σ_{nm} ($\sigma_{54}=1/1.35 \times 10^{-3} \text{ s}^{-1}$; $\sigma_{21}=1/1 \times 10^{-3} \text{ s}^{-1}$) - the probability for radiative and ρ_{nm} ($\rho_{65}=1/0.1 \times 10^{-6} \text{ s}^{-1}$; $\rho_{32}=1/0.6 \times 10^{-6} \text{ s}^{-1}$) the probability for non-radiative spontaneous transitions from level n to level m , K_{tr} ($1 \times 10^{-22} \text{ m}^3/\text{s}$) is the energy transfer coefficient between Er and Yb levels. These equations are solved using the finite differences method. The simulation allowing us to see for processes such as dynamic gain saturation, which results in the temporal reshaping of the pulse and time-dependent ASE fraction, output average and peak power. The results of the simulation and measurement for the PA1 and MA are presented in Fig. 4(a-d).

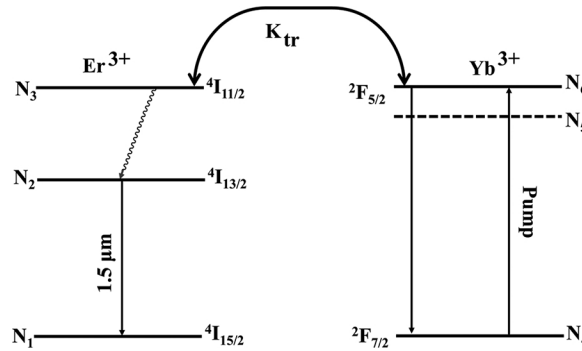


Fig. 3. Energy level diagram of the Er-Yb system.

3.1. Operation with continuous seed and pulsed pump

At first, we simulated the situation when the seed is a continuous signal at a wavelength of 1550 nm at the pulse pump with different pulse duration (color lines) also at the continuous pump (black line).

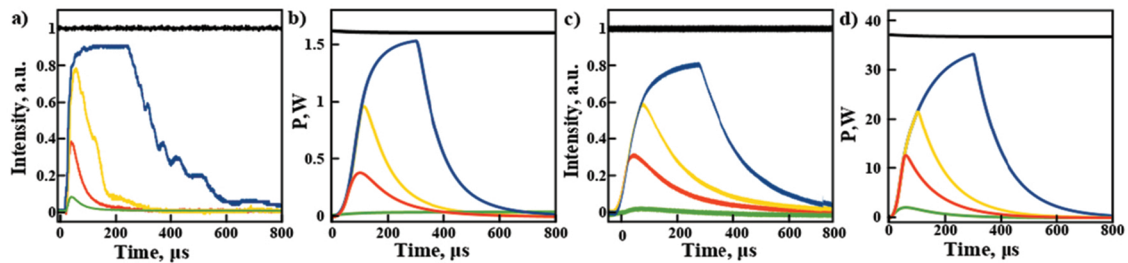


Fig. 4. The experimental (a,c) and simulation (b,d) performances of amplifiers ((a,b) - PA1, (c,d) - MA) at continuous seed and pulsed pump with duration 10 μs - green line, 50 μs (red), 100 μs (yellow), 300 μs (blue) and black line - laser operating in CW mode.

Consider the situation, for example, for the first and main amplifiers. Similar results were obtained for all preamplifiers. The black line in Fig. 4(a,c) shows the actual output average power in CW mode after 1PA and MA which corresponds power of 1.3 W and 37 W respectively and

is in good agreement with simulations Fig. 4(b,d). The black solid line (b,d) represents output power level after the system reaches steady at continuous input signal power of 95 mW for 1PA (b) and 7 W for MA (d) and continuous pump power of 4 W and 96 W for 1PA and MA respectively. The colors graphs in Fig. 4(a-d) represent the output power when the pump is sent in the form of the rectangular pulse with a duration of 300 μs , 100 μs , 50 μs , and 10 μs . The peak power of the pump was 4 W and 96 W for 1PA and MA correspondingly and the pump starts at zero time for each graph of the pulsed pump except CW (black line). For all cases with the pulsed pump, we did not obtain pulses with high peak power. As be seen, for the small pulse duration, the output peak power was too low after each stage. According to the obtained results, the steady-state in MA (Fig. 4(c,d)) at the given pump level will be reached at 500 μs after the pump starts. Also, the leading and falling edges are several hundred μs each. For the pump pulse duration with less than 300 μs , the steady-state power seems impossible to reach. The minimal output pulse duration (FWHM) which can be reached at these conditions is 50 μs , with non-rectangular pulse shape.

3.2. Operation with pulsed seed and pulsed pump

The next set of simulations and experiments were done with the pulsed seed signal, where the seed was a rectangular pulse, with different pulse duration, and sent with a different time delay with respect to the pump pulse. For example, for the results presented in Fig. 5(a) the time delay between the pump and the seed pulse was 500 μs for each case (after the amplifier reaches steady-state inversion population), the pump pulse duration was 400 μs , and the seed pulse durations were 100 μs , 50 μs , and 10 μs . Figure 5(a) shows the experimentally obtained pulses at 1 kHz after the MA at different seed pulse duration, demonstrating the significant pulse steepening at the front edge. It leads to the reduction of the average peak power over the pulse (whole pulse energy divided by the pulse duration). The black line shows the level of the output signal power in continuous mode. As an example, when we amplified μs pulses in PA1, the peak power was 70 - 80% and after the PA2 we obtained only 40 - 70 % of the expected peak power (7 W). The same behavior was observed in the final amplifier. For example, at 5 kHz and 50 μs the peak power was 15.2 W but at 500 Hz it was just 5.9 W at the same pulse duration. Increasing the pump pulse width causes additional ASE growth and does not increases the desirable peak power.

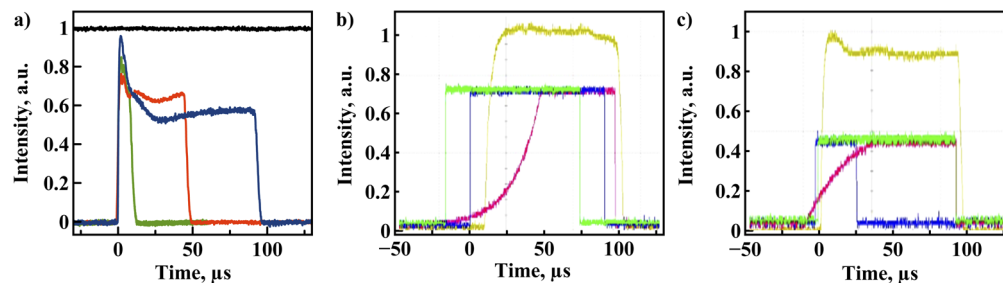


Fig. 5. The output pulses after MA at 1 kHz with pulsed seed (a) pulse steepening at different duration of the seed pulses: 10 μs (green line), 50 μs (red), 100 μs (blue), black line - laser operating in CW mode. (b,c) laser output (yellow line) for pre-shaped for seed pulse (purple line), blu and green lines are the pump pulses. All result (except of CW) the pump was pulsed.

3.3. Pulse shaping method

To find the best method, we tried to modify the shape of seed pulses before entering to the amplifiers. To determine the parameters for pulse shaping, we tested several types of input pulses.

Figure 5(b, c) shows the optimized input pulse shapes produced by the seed diode (purple line) for 100 ns output pulse. In this way, we obtained the output pulse with a square form. However, it should be noted that to get the output pulse with a square shape (yellow line) was necessary to send pump pulses with different pulse duration and sent with a different time delay concerning the seed pulse. We experimentally compared this approach with the methods described above and can note that high peak power is also difficult to reach in this case.

4. Description of the applied method in pulsed mode

As summary to the simulation and the experimental results presented above, we concluded that in order to reach stable μs pulse in the output of the system, the seed pulse must be sent to every amplifier when the inversion population is the same as for CW steady-state operation. To satisfy this condition, we added an additional seed source to the system which operates at 1560 nm (see Fig. 1). It acts as a sacrificial source when the amplifiers are reaching steady-state concerning pump and signal levels and is filtered out at the end of the system by the free-space narrow band-pass filter. The general operating principles of the proposed scheme can be seen in Fig. 6.

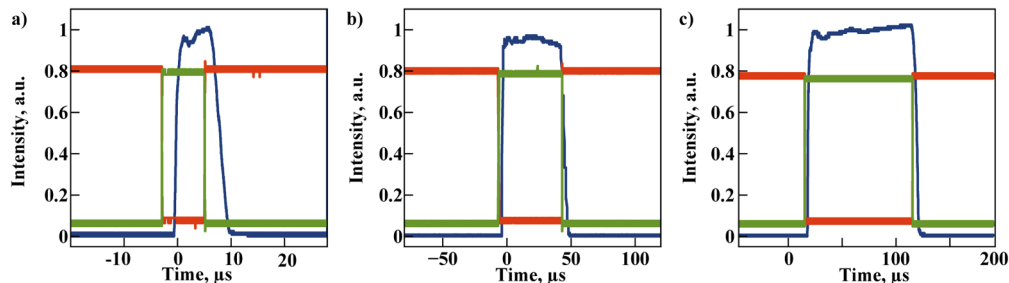


Fig. 6. The oscilloscope traces: green trace - 1550 nm seed, red trace - 1560 nm seed, blue trace - optical output pulse for, a) - 10 μs , b) - 50 μs , c) 100 μs .

The first two preamplifiers PA1 and PA2 were continuously pumped for all repetition rates of the system. The main amplifier was continuously pumped (96 W) at the repetition rates from 1 kHz to 10 kHz, and at a low repetition rate (below 1 kHz) is starting to be pumped around 1 ms prior to the expected pulse at 1550 nm arrives. The seed source at 1560 nm is working only during the pumping time (red trace in Fig. 6). It produces stimulated emission at 1560 nm instead of a broadband ASE radiation, which is effortlessly filtered out by the band-pass filter in the output of the laser. After the inversion population of the main amplifier reaches steady-state, the seed at 1560 nm is switched off and the seed at 1550 nm starts working (green trace in Fig. 6), producing the desired pulse at the output of the system (blue traces in Fig. 6). After the desired duration achieved at 1550 nm, the source at 1550 nm and the pump diodes of the main amplifier are shut down, and the seed at 1560 nm is turned on again, ensuring a sharp, almost immediate falling edge for the signal at 1550 nm.

The output spectra of the laser at different repetition rates shown in Fig. 7(a-c). As be seen in Fig. 7, in addition to the output signal at 1550 nm, the output spectrum of the final amplifier contains light at 1560 nm which also passes through the filter. The difference between the lines of the spectrum of different wavelengths is 20 dB at a low repetition rate and more than 25 dB after 1 kHz. The optical resolution of a spectrometer was 0.03 nm. At the same pump level in continuous and pulse mode (96 W), we obtained the peak power of 23-27 W at 50-500 Hz and 32 W at 1-10 kHz. The peak power is slightly lower at 10 μs and increases with increasing pulse duration. Increasing pump power in pulse mode at a low repetition rate, we can also reach peak power more than 30 W.

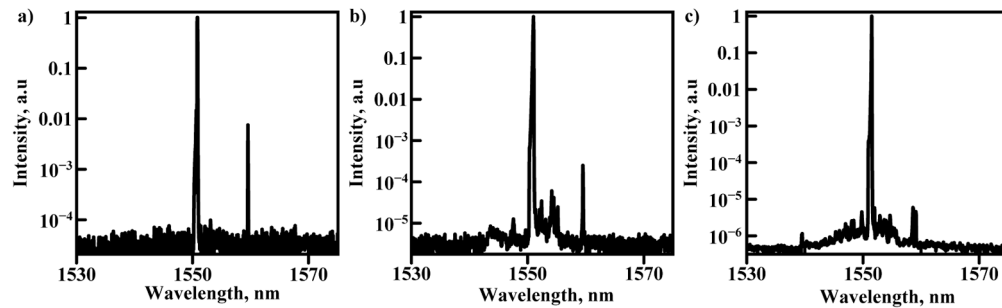


Fig. 7. Output spectra in pulsed mode after the filter: a) 20 μs at 50 Hz b) 50 μs at 1.5 kHz c) 90 μs at 10 kHz.

The system was tested at continuous operation nonstop 12 hours at full power many times, with more than 300 hours of full operation time. During this time we did not observe any visible degradation in terms of output power. The system is developed not only as a laboratory version but also as fully electronically controllable off-the-shelf product. Despite the use of large mode area gain fiber in the main amplifier, the measured beam quality is found to be $M^2=1.1$.

5. Conclusion

As a conclusion, we propose and experimentally demonstrate a new method to avoid the aforementioned pulse steepening and ASE problems. To overcome uncontrollable ASE growth at a low repetition rate and to prevent pulse steepening during the amplification, a scheme with two seed sources was used for the first time to the best of our knowledge. We have reported an all-fiber high power laser system with controllable rectangular-shape μs pulses in the range from 10 μs to 100 μs , in a wide range of repetition rates from 50 Hz to 10 kHz with peak power up to 32 W. In CW mode the system can operate at 1550 nm or 1560 nm or both wavelength at the same time with output power up to 35 W. All the system produced using commercially available components and is a fully electronically integrated product.

Acknowledgments

The authors thank, to M. Tasali.

Disclosures

The authors declare no conflicts of interest.

References

1. P. Verburg, G. Römer, and A. Huis in 't Veld, "Two-photon induced internal modification of silicon by erbium-doped fiber laser," *Opt. Express* **22**(18), 21958–21971 (2014).
2. I. Pavlov, O. Tokel, S. Pavlova, V. Kadan, G. Makey, A. Turnali, Ö. Yavuz, and F. Ö. Ilday, "Femtosecond laser written waveguides deep inside silicon," *Opt. Lett.* **42**(15), 3028–3031 (2017).
3. M. Dalponte, L. Ene, T. Gobakken, E. Næsset, and D. Gianelle, "Predicting Selected Forest Stand Characteristics with Multispectral ALS Data," *Remote Sens.* **10**(4), 586 (2018).
4. J. Yun, C. Gao, S. Zhu, C. Sun, H. He, L. Feng, L. Dong, and L. Niu, "High-peak-power, single-mode, nanosecond pulsed, all-fiber laser for high resolution 3D imaging LIDAR system," *Chin. Opt. Lett.* **10**(12), 121402 (2012).
5. Y. Jeong, S. Yoo, C. A. Codemard, J. Nilsson, J. K. Sahu, D. N. Payne, R. Horley, P. W. Turner, L. M. B. Hickey, A. Harker, M. Lovelady, and A. Piper, "Erbium:Ytterbium co-doped large core fiber laser with 297-W continuous-wave output power," *IEEE J. Sel. Top. Quantum Electron.* **13**(3), 573–579 (2007).
6. X. Bai, Q. Sheng, H. Zhang, S. Fu, W. Shi, and J. Yao, "High-Power All-Fiber Single-Frequency Erbium-Ytterbium Co-Doped Fiber Master Oscillator Power Amplifier," *IEEE Photonics J.* **7**(6), 7103106 (2015).

7. M. Jebali, J. Maran, and S. LaRochelle, "264 W output power at 1585 nm in Er–Yb codoped fiber laser using in-band pumping," *Opt. Lett.* **39**(13), 3974–3977 (2014).
8. O. De Varona, W. Fittkau, P. Booker, T. Theeg, M. Steinke, D. Kracht, J. Neumann, and P. Wessels, "Single-frequency fiber amplifier at 1.5 μm with 100W in the linearly-polarized TEM₀₀ mode for next-generation gravitational wave detectors," *Opt. Express* **25**(21), 24880–24892 (2017).
9. D. Creeden, H. Pretorius, J. Limongelli, and S. D. Setzler, "Single frequency 1560 nm Er:Yb fiber amplifier with 207 W output power and 50.5 slope efficiency," *Proc. SPIE* **9728**, 97282L (2016).
10. V. V. Dvoyrin, D. Klimentov, J. O. Klepsvik, I. V. Mazaeva, and I. T. Sorokina, "Multi-kilowatt peak power nanosecond Er-doped fiber laser," *IEEE Photonics Technol. Lett.* **28**(23), 2772–2775 (2016).
11. L. Holmen, G. Rustad, and M. Haakestad, "Robust Eye-safe Pulsed Fiber Laser Source for 3D Ladar Applications," *Appl. Opt.* **57**(23), 6760–6767 (2018).
12. J. Barria, S. Roux, J. Dherbecourt, M. Raybaut, J. Melkonian, A. Godard, and M. Lefebvre, "Microsecond fiber laser pumped, single-frequency optical parametric oscillator for trace gas detection," *Opt. Lett.* **38**(13), 2165–2167 (2013).
13. J. Nicholson, A. DeSantolo, M. Yan, P. Wisk, B. Mangan, G. Puc, A. Yu, and M. Stephen, "High energy 1572.3 nm pulses for CO₂ LIDAR from a polarization-maintaining very-large-mode-area Er-doped fiber amplifier," *Opt. Express* **24**(17), 19961–2564 (2016).
14. I. Pavlov, E. Dülgergil, E. Ilbey, and F. Ö. Ilday, "Diffraction-limited, 10-W, 5-ns, 100-kHz, all-fiber laser at 1.55 μm ," *Opt. Lett.* **39**(9), 2695–2698 (2014).
15. M. Karasek, "Optimum design of Er/sup 3+/-Yb/sup 3+/- codoped fibers for large-signal high-pump-power applications," *IEEE J. Quantum Electron.* **33**(10), 1699–1705 (1997).